

Genetic Control of Neuroadapted Sindbis Virus Replication in Female Mice Maps to Chromosome 2 and Associates with Paralysis and Mortality

DZUNG C. THACH,¹ STEVEN R. KLEEGERGER,² PAMELA C. TUCKER,^{1†} AND DIANE E. GRIFFIN^{1*}

W. Harry Feinstone Department of Molecular Microbiology and Immunology¹ and Department of Environmental Health Sciences,² Bloomberg School of Public Health, Johns Hopkins University, Baltimore, Maryland 21205-2179

Received 21 February 2001/Accepted 29 May 2001

Neuroadapted Sindbis virus (NSV) infection of mice causes hindlimb paralysis and 100% mortality in the C57BL/6 mouse strain, while adults of the BALB/cBy mouse strain are resistant to fatal encephalomyelitis. Levels of viral RNA are higher in the brains of infected C57BL/6 mice than in BALB/cBy mice (D. C. Thach et al., *J. Virol.* 74:6156–6161, 2000). These phenotypic differences between the two strains allowed us to map genetic loci involved in mouse susceptibility to NSV and to find relationships between mortality, paralysis, and viral RNA levels. Analysis of percent mortality in H2-congenic and F₁ mice suggested that the H2 locus, sex linkage, and imprinting were not involved in determining susceptibility and that resistance was partially dominant over susceptibility. Segregation analysis using CXB recombinant inbred (RI) mice indicated that the percent mortality was multigenic. Interval mapping detected a suggestive quantitative trait locus (QTL) on chromosome 2 near marker D2Mit447. Analysis of paralysis in the RI mice detected the same suggestive QTL. Viral RNA level in F₁ mice was intermediate. Interval mapping using viral RNA levels in RI mice detected a significant QTL near marker D2Mit447 that explained 69% of the genetic variance. This QTL was confirmed in F2 mice and was designated as *Nsv1*. Viral RNA level, percent paralyzed, and percent mortality were linearly correlated ($r = 0.8$ to 0.9). These results indicate that mortality, paralysis, and viral RNA levels are related complex traits and that *Nsv1* controls early viral load and determines the likelihood of paralysis and death.

Alphaviruses are positive-strand, enveloped, icosahedral viruses that cause diseases in humans ranging from encephalitis to arthritis (30). Sindbis virus (SV) is the prototype virus for this group and SV infection of mice is a model to study virus-induced neuronal cell death and immune responses in the central nervous system. Neuroadapted SV (NSV) was derived from a less virulent strain of SV (AR339) by serial passage between neonatal and adult BALB/c mice (25). While most SV strains do not cause fatal disease in adult mice, infection with NSV has a high mortality for AKR/J, A/J, C3H/HeJ, SJL/J, DBA/2J, and C57BL/6 (B6) mice, whereas BALB/cBy (Bc) mice are resistant (49).

Genetic determinants of mouse susceptibility to viral infection have been studied in many systems, mostly involving the leukemia-inducing viruses (1, 15, 27, 32–34, 37–39, 51; MGI homepage, site 1, http://www.informatics.jax.org/searches/marker_form.shtml), of which the Friend virus system is the most extensively studied. For Friend virus, resistance and susceptibility loci have been mapped for various phenotypes, such as T-cell response, neutralizing antibody, and virus replication, in various strains of mice, followed by fine mapping and candidate gene analysis or functional cloning (5, 26, 28, 31, 46, 47). Studies of virus interaction with cells derived from these mice also helped to elucidate the actions of resistant or susceptible

alleles (5, 46). Several genes have been cloned, including *Fv1* and *Fv4*, which turned out to be genes derived from endogenous retroviruses that interfere with the replication of related exogenous retroviruses (28, 31, 46). Among the non-leukemia-inducing viruses, loci involved in susceptibility or resistance have been identified or mapped for the control of cytomegalovirus splenic replication by natural killer (NK) cells (*Cmv1* [8, 9, 20–22, 24, 40–43]), hepatitis virus replication in macrophages and neurons (*Hv1* and *Hv2*), flavivirus-induced lethality (*Fhv*), Japanese encephalitis virus (*Jevr*), Newcastle disease virus-induced interferon (*If1*), influenza virus resistance (*Mx1*), and others (MGI homepage, site 1). Most of these traits are ascribed to single genes and are mendelian in character. Variability in susceptibility to virus infection in other systems, such as mousepox (10–13, 19, 29) and Theiler's murine encephalomyelitis virus (TMEV) infection (2, 3, 6, 7, 16–18, 35), are complex and quantitative traits. In mousepox, infection mortality is a dominant phenotype, and genetic dissection strategies have included genome scans and congenic mice (14) to identify the loci involved. The discovered loci led to candidate gene NK cell receptor NKR-P1 and the fifth component of complement, which are involved in viral pathogenesis (14). For TMEV, the phenotype studied was persistent viral RNA in the spinal cords of infected mice, and several loci were found to associate with viral RNA level. Again, the discovered loci led to candidate genes: gamma interferon and *H-2D*, which are involved in viral persistence (3, 4, 23).

In 5-week-old B6 and Bc mice infected intranasally (i.n.), NSV infects neurons of the olfactory region and spreads caudally. Virus replication and spread is faster in B6 mice than in Bc mice, causing paralysis and 100% mortality in B6 mice,

* Corresponding author. Mailing address: W. Harry Feinstone Department of Molecular Microbiology and Immunology, Johns Hopkins University, Bloomberg School of Public Health, 615 N. Wolfe St., Baltimore, MD 21205. Phone: (410) 955-3459. Fax: (410) 955-0105. E-mail: dgriffin@jhsph.edu.

† Deceased.

whereas Bc mice survive infection (48). These differing traits—virus replication, percent paralysis, and percent mortality—can be used to identify loci involved in susceptibility to NSV infection. These traits are similar to the phenotypes of other viral systems, but the genetic basis of NSV susceptibility is probably different from other viral infections because of differences in the pathogenesis and in the susceptibility patterns of various inbred strains. In this study, we used the B6 and Bc strains as parents and the percent mortality, percent paralysis, and viral RNA level as phenotypes. For one or all traits, we determined the role of the *H2* locus; the presence or absence of sex specificity, sex-linked or imprinted loci, and dominance, and we performed a genome scan using recombinant inbred (RI) mice with confirmation of detected loci using F_2 mice. Finally, we looked at the relationship between mortality, paralysis, and viral RNA levels.

MATERIALS AND METHODS

Animals and virus. C57BL/6, C57BL/6ByJ, BALB/cBy, B6.C-H2^d/bBy, CByB6F1/J, and CXB RI mice were purchased from The Jackson Laboratory (Bar Harbor, Maine). (C57BL/6 × BALB/cBy) F_1 and (CByB6F1 × CByB6F1) F_1 (F_{2S} of Bc and B6 mice) mice were bred and raised at the Johns Hopkins University pathogen-free animal facilities in microisolator cages. Mice were anesthetized with methoxyflurane (Schering-Plough), and a pipette was used to deliver drops of inhalable virus solution to the left nostril. The NSV strain of SV (25) was grown and assayed in BHK-21 cells and 2.4×10^4 PFU were delivered to each mouse in 15 μ l of Hanks balanced salt solution (HBSS) with HEPES (51:1).

Intracerebral (i.c.) inoculation was used for some mortality measurements in CXB RI mice. In this case, 1,000 PFU were delivered in 30 μ l of HBSS and HEPES using 25G tuberculin syringes (Becton Dickinson). Previous studies showed that intracerebral and intranasal inoculation with NSV results in comparable mortality (48).

Probes. Nucleotides 8638 through 8912 (E2 coding region) were amplified by PCR from the 633 SV clone (50) and cloned into pGEM-3Z vector (Promega). Digoxigenin (DIG)-labeled RNA probes were made by *in vitro* transcription with DIG-UTP (Boehringer Mannheim) from the SP6 promoter after plasmid linearization with *EcoRI*.

Nucleotides 236 through 1034 were amplified by PCR from GAPDH (glyceraldehyde-3-phosphate dehydrogenase) cDNA from B6 mice and cloned into pGEM-3Z vector. To make a 282-nucleotide probe, primers 5'-CGACGTTGT AAAACGACGGC-3' and 5'-GACACCAAGGAGATGGTGAAGCAG-3' were used to amplify a region from the plasmid spanning the T7 promoter site and part of the GAPDH insert (36, 45). The PCR product was isolated using Gene-Clean II Kit (Bio 101) and was used to make DIG-labeled RNA probes as described above.

Dot blot. The left half of the brain was removed from phosphate-buffered saline-perfused mice, homogenized in RNA-Stat (Tel-Test, Friendswood, Tex), frozen on dry ice, and stored at -80°C for no more than 2 weeks. RNA was extracted with chloroform, precipitated with isopropanol, washed with 70% ethanol, spun down, dried, and resuspended in diethyl pyrocarbonate-treated water. The samples were adjusted to 2 μ g of total RNA per μ l based on optical density (OD) measurements.

One μ l from each sample was dotted onto Hybond N+ (Amersham) membranes, UV cross-linked, and baked for 30 min at 80°C . Virus and GAPDH-specific RNAs were detected using the appropriate probes and methods as described by Shifman and Stein (44). Briefly, the membranes were prehybridized at 68°C for 3 h, hybridized overnight, and washed three times. The membranes were blocked with 2% Boehringer Mannheim blocking reagent in modified maleate buffer, incubated with alkaline phosphatase-conjugated antibody, followed by disodium 3-(4-methoxyphosphoryl)-5-chloro-2-tricyclo[3.3.1.3^{3,7}](decan-4-yl)phenyl phosphate (CSPD) chemiluminescent substrate (Boehringer Mannheim), and detected on Hyperfilm ECL (Amersham) films. Uncalibrated OD (uOD) measurements used NIH Image software (NIH Image, <http://rsb.info.nih.gov/nih-image/index.html>).

Genotyping. To extract DNA, half spleens were homogenized in DNAzol (Gibco-BRL), and DNA was precipitated with 100% ethanol, spooled, washed twice with 95% ethanol, and solubilized with either TE (pH 8.0) alone or 8 mM NaOH followed by neutralization with HEPES.

TABLE 1. Strain distribution patterns of 13 CXB RI strains for various markers^a

Chromosome	Locus	Strain distribution patterns		
		12345	67891 0	111 123
2	D2Mit104	cbbcb	bbccc	ccb
	D2Mit410	cccb	bbbcc	cbb
	D2Mit447	cbbcb	bbccb	ccb
6	D6Mit301	bbccc	bcccc	ccc
9	D9Mit166	ccccc	bcccb	bbb
	D9Mit215	cbbbb	bcccb	ccb

^a The Bc allele is c; the C57BL/6By allele is b.

To label primers for one PCR reaction, we mixed 1.8 μ l of 5 \times buffer (0.25 M Tris, pH 9; 0.05 M MgCl₂; 0.05 M dithiothreitol; 0.25 mg/ml), 3.3 μ l of MapPairs (Research Genetics) forward primer (6.6 μ M), 10 U of polynucleotide kinase (Roche), 2 μ l of [γ -³²P]ATP (10 μ Ci/ μ l; 6,000 Ci/mmol), and H₂O to a total of 10.15 μ l. The reaction was incubated at 37°C for 1 h, and an equal volume of water was added. The labeled primer was isolated by passing the mixture through a P4-Bio-Gel resin (Bio-Rad) Select D spin column (Eppendorf).

For one PCR reaction, we mixed 3 μ l of DNA (60 to 80 ng), 1.25 μ l of 10 \times reaction buffer (500 mM KCl; 100 mM Tris, pH 8.3; 15 mM MgCl₂), 0.25 μ l of deoxynucleoside triphosphates at 10 mM (equal volumes of dATP, dGTP, dTTP, and dCTP, 2.5 mM each), 0.5 μ l of unlabeled primer (Research Genetics) (6.6 μ M), 0.075 μ l of *Taq* polymerase (5 U/ μ l), 0.127 μ l of labeled primer (The ratio of labeled to unlabeled primer is 0.15), and double-distilled water to a total of 12.5 μ l. Thermocycler conditions were as follows: 94°C for 5 min, followed by 30 or more cycles of 94°C for 30 s (denaturation), 55°C for 30 s (annealing), 72°C for 30 s (elongation), depending on efficiency of primers, then 72°C for 7 min, and 4°C for storage. PCR products were resolved on 6% acrylamide gels.

Statistical analysis. StatView (SAS Institute, Cary, N.C.) was used to analyze results for statistical significance. The percent mortality was calculated as the proportion of mice that died between days 0 and 14 for *i.n.* infection and between days 5 and 12 for *i.e.* infection, multiplied by 100. The percent mortalities in F_1 mice were compared using hypothesis testing on proportions.

For the RI mouse strains, the percent mortality was the average of three experiments: 5-week-old mice infected *i.n.* ($n = 7$ to 8) or *i.c.* ($n = 9$ to 14), and 10.6-week-old mice infected *i.c.* ($n = 10$ to 17). This gave the most accurate estimation of the true percent mortality of each RI strain. Map Manager (K. Manly, <http://mcbio.med.buffalo.edu/mapmgr.html>) was used to perform a genome scan, and interval mapping with the RI mice phenotyped for percent mortality was used as a quantitative trait. Briefly, a genome scan is an experimental design in which, for a cohort of mice, such as the RI mouse strains, traits are measured and markers spaced throughout the genome are genotyped. Interval mapping is a mathematical model that uses data from the genome scan to quantitate the strength of association between traits and markers by calculation of the likelihood ratio statistic (LRS). The significance of association between traits and markers was determined by the permutation test set at 1,000 permutations using Map Manager. Briefly, the permutation test randomizes the trait values a thousand times and determines the maximum LRS of the randomized trait values and markers each time. The maximum LRSs generated form an empirical density distribution similar to the theoretical χ^2 distribution that can be used for testing the significance of the LRSs from the original trait values. Marker strain distribution patterns for the CXB RI set were obtained from the Map Manager package (MGI homepage, site 2, http://www.informatics.jax.org/searches/riset_form.shtml), and some were genotyped by our laboratory (Table 1). The map used for analysis totaled 228 unique markers with no uninformative loci.

A subset of the mice observed for mortality was observed for hind-limb paralysis before death. The percent paralysis for each mouse strain is quantitated as the pooled proportion of paralyzed mice observed divided by the total observed. The analysis of the percent paralysis is similar to that for the percent mortality.

For F_1 and F_2 mice, viral RNA was quantitated as the ratio of viral RNA uOD to GAPDH uOD (Fig. 1). Viral RNA in the RI mice was quantitated as the log of [(viral RNA in picograms/GAPDH in picograms) \times mean GAPDH level in picograms], where the brightness of each dot was converted to picograms via

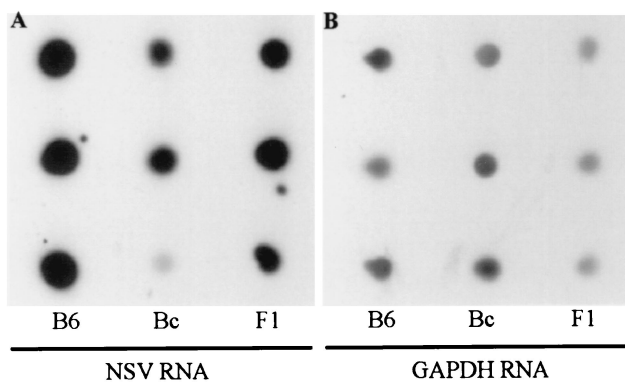


FIG. 1. Dot blot quantitation of viral RNA phenotype. (A) Sample blot of RNA extracted from brain 4 days after infection hybridized with an NSV-specific probe showing high, low, and medium signals in three B6, Bc, and F₁ mice, respectively. (B) Corresponding GAPDH blot.

standard curves. A genome scan and interval mapping were performed for mean viral RNA in the same manner as for the percent mortality. Differences in viral RNA among the marker genotypes of the F₂ mice were analyzed by using one-way analysis of variance (ANOVA). All viral RNA quantitative analysis was done for dots from the same Hybond N+ membrane.

Relations between the percent mortality, the percent paralysis, and the viral RNA level in the RI mice were analyzed using the Pearson correlation coefficient and the Fisher *r*-to-*z* transformation test. Statistical significance was accepted at a *P* of <0.05.

RESULTS

Mortality and paralysis. (i) Role of H2 locus in mortality.

Since the *H2* locus is involved in susceptibility to many infectious diseases, we determined the genetic role of the *H2* locus on mortality by assessing the survival in eight female 5- to 10-week-old B6.C-H2^d/bBy congenic mice (Bc *H2* on a B6 background). There was 100% mortality in both the congenic and the B6 strains, suggesting that *H2* was not genetically involved in determining mortality.

(ii) Analysis of the percent mortality in the F₁ mice.

To determine the presence or absence of sex specificity, sex-linked or imprinted loci, and dominance, we measured the percent mortality in male and female (C57BL/6 × BALB/cBy)F₁ mice and its reciprocal: CByB6F₁/J mice (Table 2). There were no statistically significant differences in mortality between the reciprocal F₁ mice or between the sexes, suggesting that there were no sex-linked or imprinted loci and no sex specificity. Thus, all F₁ mice were pooled together to estimate the true

TABLE 2. Analysis of percent mortality in F₁ mice

Group	Sex	% Mortality	<i>n</i>	<i>P</i> ^a
(Bc × B6)F ₁	M	46	24	0.14 ^b
(B6 × Bc)F ₁	M	29	45	
(Bc × B6)F ₁	F	29	24	0.96 ^c
(B6 × Bc)F ₁	F	30	47	
Male F ₁	M	35	69	0.51 ^d
Female F ₁	F	30	71	
Pooled F ₁		32	140	

^a Based on hypothesis testing on proportions.

^b Comparing male reciprocals.

^c Comparing female reciprocals.

^d Comparing males to females of pooled reciprocals.

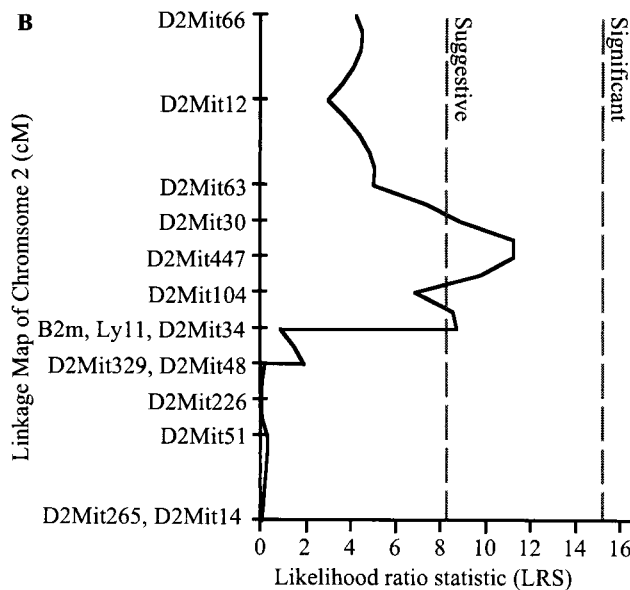
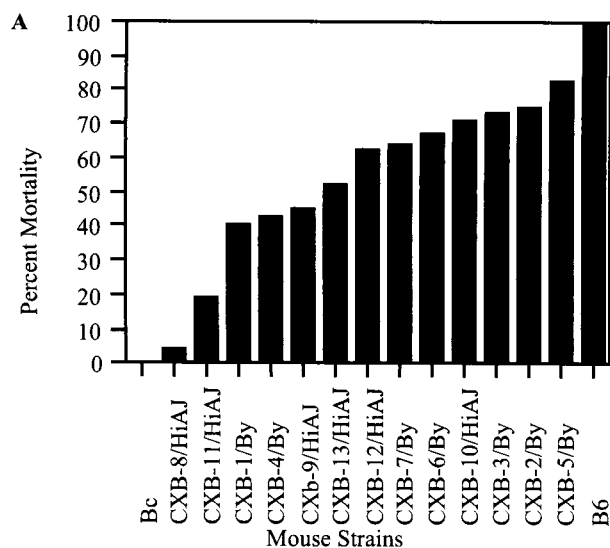


FIG. 2. NSV-induced mortality of recombinant inbred and parental strains of mice. (A) Average percent mortality in B6, Bc, and CXB RI mice (*n* = 26 to 39). (B) Interval mapping of percent mortality on chromosome 2. Suggestive and significance levels were determined by the permutation test. The marker D2Mit66 is centromeric.

percent mortality to be 32%. This was different from that of both parents (*P* < 0.05), with resistance being partially dominant over susceptibility.

(iii) Analysis of the percent mortality in RI mice. To map loci involved in the percent mortality, a genome scan was done using the average percent mortality of female CXB RI mice infected with NSV. If one qualitative gene were involved in the percent mortality, then one would expect a 1:1 ratio of susceptible to resistant strains in the strain distribution pattern of the RI mice. This was not the case, indicating that mortality was multigenic (Fig. 2A). Interval mapping of the percent mortality as a quantitative trait detected a suggestive quantitative trait locus (QTL) near marker D2Mit447 (60.1 centimorgans [cM] on the MGD map [36]) on chromosome 2 (Fig. 2B). Both B6

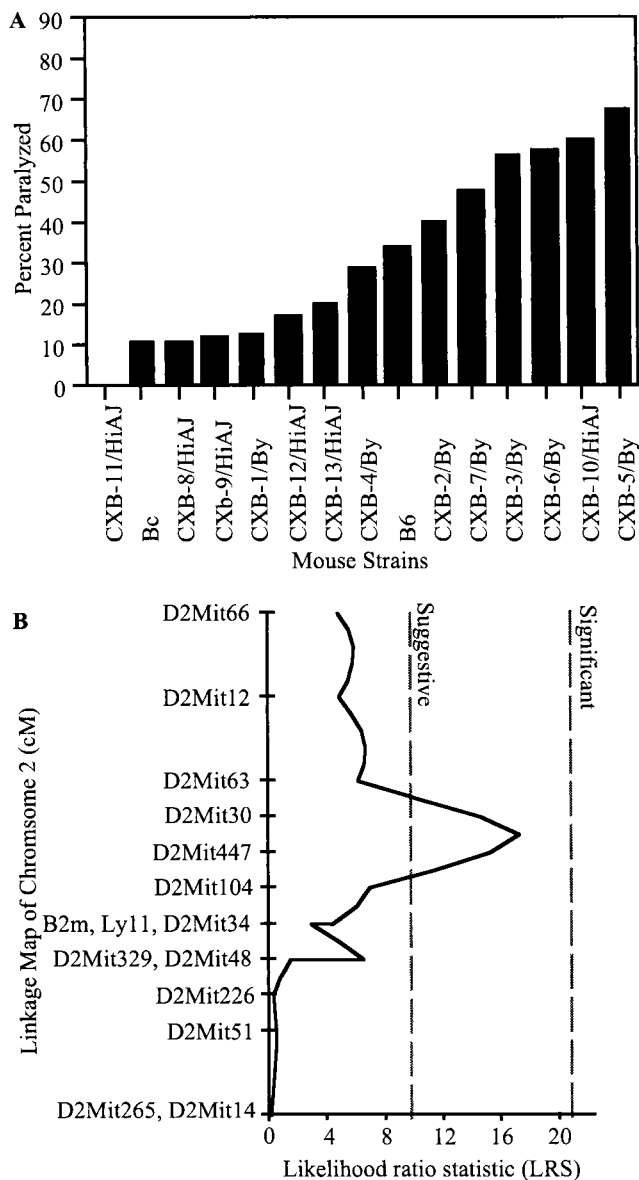


FIG. 3. NSV-induced paralysis in recombinant inbred and parental strains of mice. (A) Percent paralyzed in B6, Bc, and CXB RI mice ($n = 23$ to 47). (B) Interval mapping of percent paralyzed on chromosome 2. Suggestive and significance levels were determined by the permutation test. Marker D2Mit66 is centromeric.

and C57BL/6ByJ mice showed 100% mortality after NSV infection; therefore, we have used the B6 phenotypes for comparisons with RI phenotypes.

(iv) Analysis of the percent paralysis in RI mice. Analysis of the percent paralysis yielded results similar to those of the percent mortality (Fig. 3).

Viral RNA. **(i) Role of H2 locus in viral RNA level.** To determine the role of the H2 locus in viral RNA levels, we compared viral RNA levels at day 4 postinfection of female B6.C-H2^d/bBy and B6 mice (see Fig. 5A). There was no difference in the viral RNA level between the congenic and B6 mice, suggesting that H2 was not involved in determining the level of viral RNA early after infection.

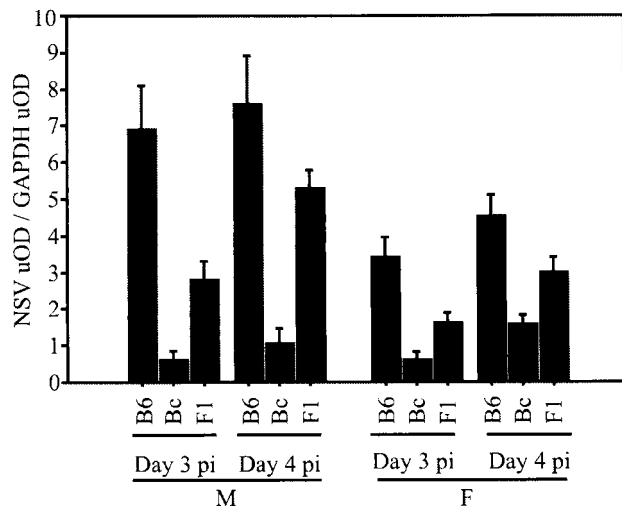


FIG. 4. Viral RNA levels compared to GAPDH RNA levels in B6, Bc, and CByB6F1 mice at 3 and 4 days after infection in male and female mice. Each bar shows mean \pm the standard error of the mean (SEM) of three to six mice.

(ii) Analysis of viral RNA level in F₁ mice. To determine the presence or absence of sex specificity and dominance, we measured viral RNA levels in CByB6F1/J mice at days 3 and 4 postinfection (Fig. 4). Males had higher viral RNA levels than females, and day 4 levels were higher than day 3 levels, as expected from infectious virus growth curves (48). RNA levels in the F₁ mice were between the parent strains in all cases. The results suggested that there was sex specificity and that viral RNA level was codominant.

(iii) Analysis of viral RNA level in RI and F₂ mice. To map loci involved in determining viral RNA level, a genome scan was done using 5-week-old female CXB RI mice infected with NSV i.n. (Fig. 5A). The distribution pattern of the 13 RI strains indicated that the trait was multigenic, and interval mapping of viral RNA level as a quantitative trait detected a significant QTL near marker D2Mit447 (60.1 cM) on chromosome 2 that explained 69% of the genetic variation (Fig. 5B). To determine if additional minor loci were detectable, we controlled for marker D2Mit447 and scanned the genome for additional loci. We detected one near marker D7Mit223 (72.4 cM) (MGI homepage, site 1) that explained 30% of the genetic variation. Another locus near marker D17Tu42 (20.43 cM) (MGI homepage, site 1) explaining 27% of the genetic variation was negatively associated.

To confirm the major QTL detected in the RI, we determined whether viral RNA levels at day 3 postinfection were significantly associated with marker D2Mit447 (60.1 cM) in F₂ mice (Fig. 6). The QTL was confirmed in F₂ mice ($P < 0.05$), but only in female mice. Nearby markers that were significantly associated with RNA levels in female F₂ mice included D2Mit164 (71.0 cM [MGI homepage, site 1], $P = 0.047$) and D2Mit104 (66.0 cM [MGI homepage, site 1], $P = 0.030$). The association of marker D2Mit410 (78.7 cM [MGI homepage, site 1], $P = 0.181$) was not significant. Analysis using the recessive regression model in Map Manager showed that the major QTL explained 8% of the variation in F₂ mice. There were not enough female F₂ mice to confirm the minor QTL.

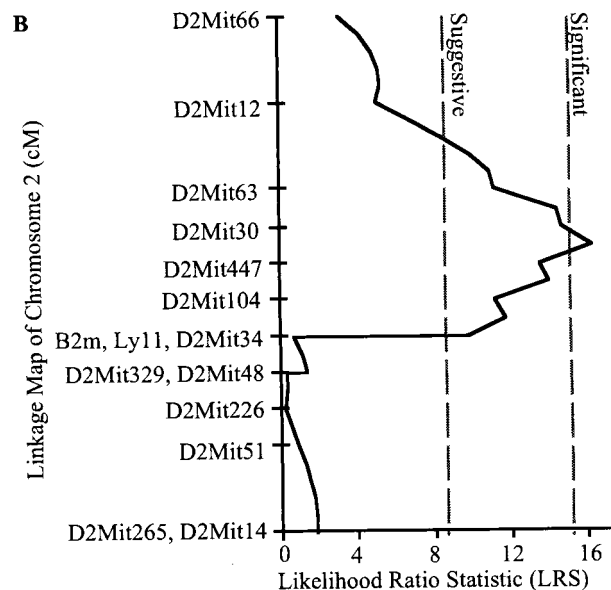
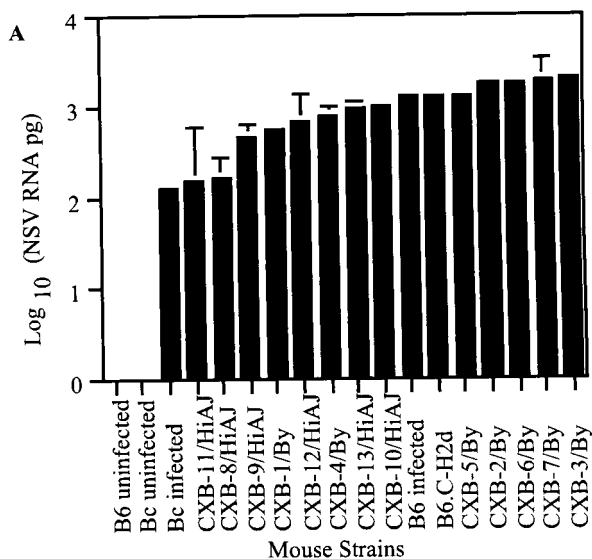


FIG. 5. (A) Viral RNA level in uninfected parents, infected parents, *H2* congenic mice, and CXB RI mice. Each bar shows the mean \pm the SEM of three mice. (B) Interval mapping of viral RNA levels on chromosome 2. Suggestive and significance levels were determined by the permutation test. The marker D2Mit66 is centromeric.

(iv) **Relationship between mortality, paralysis, and viral RNA.** The viral RNA level strongly correlated linearly with the percent mortality and the percent paralysis (Fig. 7).

DISCUSSION

We have evaluated the genetic contribution to three phenotypic differences between B6 and Bc mice after NSV infection: percent mortality, percent paralysis, and level of viral RNA in the brain early after infection. Percent mortality was an incomplete-penetrant, incomplete-dominant, multigenic trait with no evidence for sex linkage, sex specificity, imprinting, or *H2* locus involvement. Viral RNA level was a similar trait but did show sex specificity. We detected a suggestive QTL on chromosome

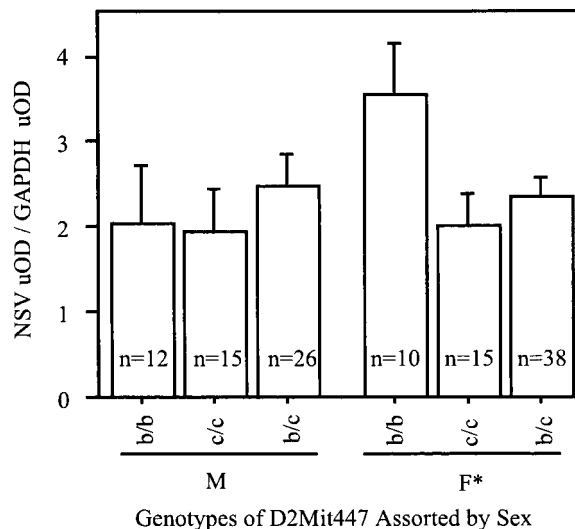


FIG. 6. Viral RNA levels of F_2 mice sorted by sex and genotypes of marker D2Mit447. The means \pm the SEM are presented. The B6 allele is b; the Bc allele is c. (For consistency with the RI mice in Table 1, we have used “b” and “c” as allelic designations for the B6 and Bc alleles, respectively. However, these alleles are designated “d” for B6 and “b” for Bc alleles in the Mouse Genome Informatics database.) *, $P < 0.05$ (ANOVA).

2 involved in determining the percent mortality and percent paralysis, and the same locus was significantly involved in determining viral RNA level in female mice. The percent mortality, percent paralyzed, and viral RNA level values were strongly correlated. These observations showed that mortality, paralysis, and viral RNA were related complex traits. The major QTL detected will allow us to identify and test candidate genes involved in NSV susceptibility.

The RI data are consistent with a two-locus model to explain differences in NSV susceptibility. There were two RI strains, CXB-8/HiAJ and CXB-11/HiAJ, that resembled the Bc parent and at least four RI strains that resembled the B6 parent. If one postulates that two independent loci are involved, then 3.25 RI strains would be expected to have one parental phenotype. Thus, the observed frequency is not very different from the expected frequency of two independent loci. Also, in the quantitative analysis of viral RNA level in the RI strains, two QTLs were detected (D2Mit447 and D7Mit223) that together explained 99% of the genetic variation. However, the major QTL detected in the RI set only explained 8% of the variation in the F_2 mice. This was not surprising since in the F_2 cohort, the total variation includes not only additive genetic factors but also heterozygosity and environmental factors. The last two factors are not present in the RI cohort because heterozygosity was removed by inbreeding, and environmental variation was removed by analyzing the mean viral RNA level. Thus, the complexity of the viral RNA trait seems to be mainly due heterozygosity and environmental factors.

The strong correlation between viral RNA level and the percent mortality suggests that viral RNA is the underlying continuous trait that induces mortality in a mouse when the RNA level exceeds a certain threshold. This seems to explain the incomplete penetrance of mortality. Quantitatively, the range of percent mortality corresponds to a 1-log range of viral

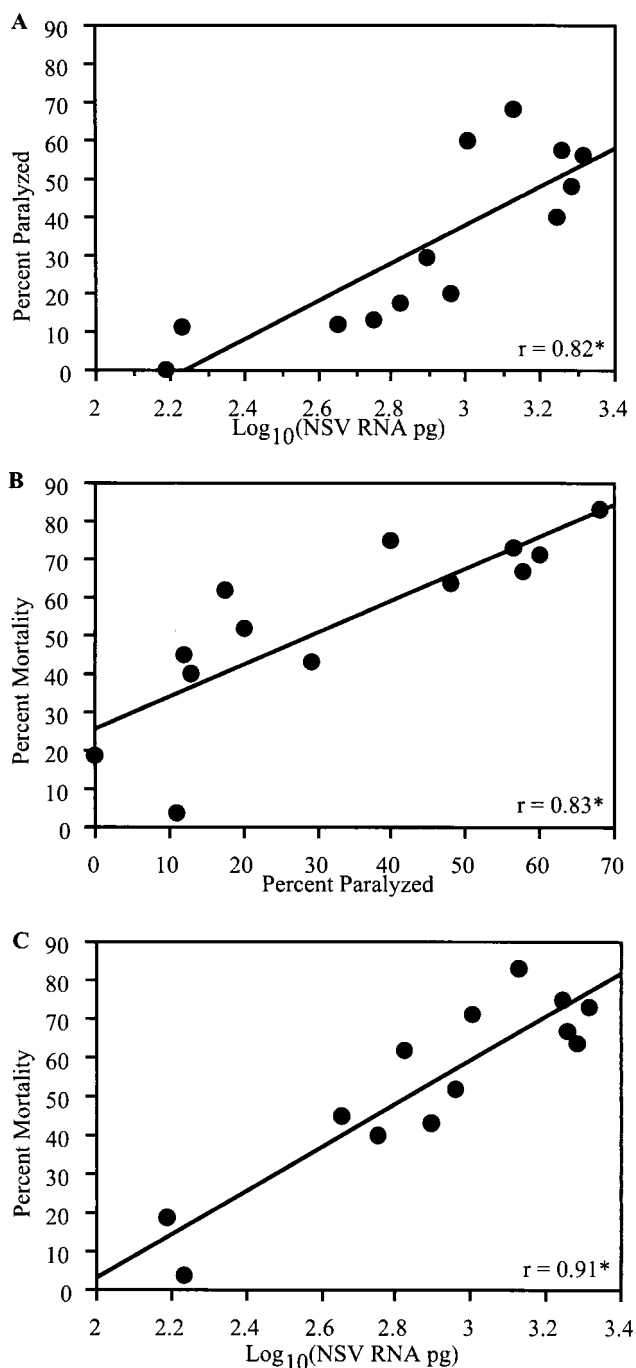


FIG. 7. Bivariate plots of percent-paralyzed versus viral RNA level (A), percent mortality versus percent paralyzed (B), and percent mortality versus viral RNA (C) of CXB RI mice. *, $P < 0.05$ (r -to- z transformation test).

RNA (Fig. 7C). The strong correlation between viral RNA level in the brain and the percent paralysis suggests that high virus replication in the brain indicates high virus replication in the motor neurons of the ventral horn in the lumbar spinal cord. The level of viral RNA in the lumbar cord then induces hind-limb paralysis with corresponding severity. The major locus on chromosome 2 was significant for viral RNA but was only suggestive for percent mortality and percent paralysis.

This is probably due to loss of information as one moves from a continuous trait, i.e., viral RNA, to a binary trait, i.e., mortality and paralysis. Also, more biologic steps are required for paralysis and mortality, suggesting that additional minor loci may be involved. The correlation between paralysis and mortality is likely due to their correlations with viral RNA. Paralysis is unlikely to be the primary cause of mortality since there were mice that were paralyzed but did not die.

Sex-specific QTLs have been found in genetic dissections of susceptibility to other viral diseases, such as the TMEV RNA level (2) and mousepox-induced mortality (10–13, 19). In the mousepox model, the reason for the sex specificity of QTL is that these QTLs are dependent on gonadal factors for their functions. Our QTL detected in females could mean that the QTL shows its effects only in the presence of female sex hormones or in the absence of male sex hormones or that more loci are involved in the males but that we were unable to detect them. The absence of sex specificity in the percent mortality may simply be due to the lower sensitivity of detection compared to viral RNA measurements, although we often observed more severe signs in male than in female mice.

In terms of pathogenesis, the B6 allele seems to allow for high virus replication in certain neuronal populations that include the motor neurons, which in turn determines greater spread, thereby compromising more neuronal functions that may be exacerbated by the specific immune response and leading to paralysis or death. The Bc allele can control virus replication. Differences in virus replication in the brain are seen as early as day 1 postinfection (48); thus, we hypothesized that candidate genes affect either innate immune response mechanisms or the development of neurons so that the neurons of B6 mice support virus replication better than the neurons of Bc mice. Adaptive immune response genes are unlikely candidates since they are involved during the clearance phase of viral infection. However, adaptive immune responses may be effectors of disease since mice with a high early viral load begin to show disease signs during the adaptive immune response. Our major QTL mapped near marker D2Mit447. Some interesting genes map to this region, including FK506 binding protein 7 (*Fkbp7*); follicle-stimulating hormone beta (*Fshb*); potassium voltage-gated channel, shaker-related (*Kcna4*); synaptosomal associated protein, 23kD (*Snap23*); biliverdin reductase (*Bhr*); cholinergic receptor, muscarinic 5 (*Chrm5*); catalase 1 (*Cas1*); recombination activating genes 1 and 2 (*Rag1* and *Rag2*); and brain-derived neurotrophic factor (*Bdnf*) (Mouse Genome Informatics, http://www.informatics.jax.org/searches/linkmap_form.shtml). We are currently evaluating BDNF as a candidate gene.

In summary, we have genetically characterized the traits of percent mortality, percent paralysis, and viral RNA level and their relationships. We have found a major QTL controlling viral RNA level that we designated *Nsv1*. These results help us to better understand the genetic differences between B6 and Bc mice in susceptibility to NSV infection and the determinants of susceptibility to neuronal infection and fatal paralytic disease.

ACKNOWLEDGMENTS

We thank David Brownstein and Roger Reeves for helpful advice, Rob Williams for his high-density CXB map, and Anne Jedlicka and Kiana Brunson for technical assistance.

This work was supported by a research grant from the Muscular Dystrophy Association (D.E.G.) and a training grant (AI07417) from the National Institutes of Health (D.C.T.). S.R.K. was supported by ES09606 and EPAR827624.

REFERENCES

- Amari, N. M., S. Kamiura, and D. Meruelo. 1990. Effects of fractionated x-irradiation on the Ly-6-Ril-1-Pol-5 region. *Immunogenetics* **32**:252–262.
- Aubagnac, S., M. Brahic, and J. F. Bureau. 1999. Viral load and a locus on chromosome 11 affect the late clinical disease caused by Theiler's virus. *J. Virol.* **73**:7965–7971.
- Azoulay, A., M. Brahic, and J. F. Bureau. 1994. FVB mice transgenic for the H-2Db gene become resistant to persistent infection by Theiler's virus. *J. Virol.* **68**:4049–52.
- Azoulay-Cayla, A., S. Dethlefs, B. Perarnau, E. L. Larsson-Sciard, F. A. Lemonnier, M. Brahic, and J. F. Bureau. 2000. H-2D(b-/-) mice are susceptible to persistent infection by Theiler's virus. *J. Virol.* **74**:5470–5476.
- Best, S., P. R. Le Tissier, and J. P. Stoye. 1997. Endogenous retroviruses and the evolution of resistance to retroviral infection. *Trends Microbiol.* **5**:313–318.
- Bihl, F., M. Brahic, and J. F. Bureau. 1999. Two loci, *Tmevp2* and *Tmevp3*, located on the telomeric region of chromosome 10, control the persistence of Theiler's virus in the central nervous system of mice. *Genetics* **152**:385–392.
- Brahic, M., and J. F. Bureau. 1998. Genetics of susceptibility to Theiler's virus infection. *Bioessays* **20**:627–633.
- Brown, M. G., S. Fulmek, K. Matsumoto, R. Cho, P. A. Lyons, E. R. Levy, A. A. Scalzo, and W. M. Yokoyama. 1997. A 2-Mb YAC contig and physical map of the natural killer gene complex on mouse chromosome 6. *Genomics* **42**:16–25.
- Brown, M. G., J. Zhang, Y. Du, J. Stoll, W. M. Yokoyama, and A. A. Scalzo. 1999. Localization on a physical map of the NKC-linked Cmv1 locus between Ly49b and the Prp gene cluster on mouse chromosome 6. *J. Immunol.* **163**:1991–1999.
- Brownstein, D., P. N. Bhatt, and R. O. Jacoby. 1989. Mousepox in inbred mice innately resistant or susceptible to lethal infection with ectromelia virus. V. Genetics of resistance to the Moscow strain. *Arch. Virol.* **107**:35–41.
- Brownstein, D. G., P. N. Bhatt, L. Gras, and T. Budris. 1992. Serial backcross analysis of genetic resistance to mousepox, using marker loci for Rmp-2 and Rmp-3. *J. Virol.* **66**:7073–7079.
- Brownstein, D. G., P. N. Bhatt, L. Gras, and R. O. Jacoby. 1991. Chromosomal locations and gonadal dependence of genes that mediate resistance to ectromelia (mousepox) virus-induced mortality. *J. Virol.* **65**:1946–1951.
- Brownstein, D. G., and L. Gras. 1995. Chromosome mapping of Rmp-4, a gonad-dependent gene encoding host resistance to mousepox. *J. Virol.* **69**:6958–6964.
- Brownstein, D. G., and L. Gras. 1997. Differential pathogenesis of lethal mousepox in congenic DBA/2 mice implicates natural killer cell receptor NKR-P1 in necrotizing hepatitis and the fifth component of complement in recruitment of circulating leukocytes to spleen. *Am. J. Pathol.* **150**:1407–1420.
- Buller, R. S., A. Ahmed, and J. L. Portis. 1987. Identification of two forms of an endogenous murine retroviral *env* gene linked to the *Rmcf* locus. *J. Virol.* **61**:29–34.
- Bureau, J. F., K. M. Drescher, L. R. Pease, T. Vikoren, M. Delcroix, L. Zoecklein, M. Brahic, and M. Rodriguez. 1998. Chromosome 14 contains determinants that regulate susceptibility to Theiler's virus-induced demyelination in the mouse. *Genetics* **148**:1941–1949.
- Bureau, J. F., X. Montagutelli, F. Bihl, S. Lefebvre, J. L. Guenet, and M. Brahic. 1993. Mapping loci influencing the persistence of Theiler's virus in the murine central nervous system. *Nat. Genet.* **5**:87–91.
- Bureau, J. F., X. Montagutelli, S. Lefebvre, J. L. Guenet, M. Pla, and M. Brahic. 1992. The interaction of two groups of murine genes determines the persistence of Theiler's virus in the central nervous system. *J. Virol.* **66**:4698–4704.
- Delano, M. L., and D. G. Brownstein. 1995. Innate resistance to lethal mousepox is genetically linked to the NK gene complex on chromosome 6 and correlates with early restriction of virus replication by cells with an NK phenotype. *J. Virol.* **69**:5875–5877.
- Depatie, C., A. Chalifour, C. Pare, S. H. Lee, S. M. Vidal, and S. Lemieux. 1999. Assessment of Cmv1 candidates by genetic mapping and in vivo antibody depletion of NK cell subsets. *Int. Immunol.* **11**:1541–1551.
- Depatie, C., S. H. Lee, A. Stafford, P. Avner, A. Belouchi, P. Gros, and S. M. Vidal. 2000. Sequence-ready BAC contig, physical, and transcriptional map of a 2-Mb region overlapping the mouse chromosome 6 host-resistance locus Cmv1. *Genomics* **66**:161–174.
- Depatie, C., E. Muise, P. Lepage, P. Gros, and S. M. Vidal. 1997. High-resolution linkage map in the proximity of the host resistance locus Cmv1. *Genomics* **39**:154–163.
- Fiette, L., C. Aubert, U. Muller, S. Huang, M. Aguet, M. Brahic, and J. F. Bureau. 1995. Theiler's virus infection of 129Sv mice that lack the interferon alpha/beta or interferon gamma receptors. *J. Exp. Med.* **181**:2069–2076.
- Forbes, C. A., M. G. Brown, R. Cho, G. R. Shellam, W. M. Yokoyama, and A. A. Scalzo. 1997. The Cmv1 host resistance locus is closely linked to the Ly49 multigene family within the natural killer cell gene complex on mouse chromosome 6. *Genomics* **41**:406–413.
- Griffin, D. E., and R. T. Johnson. 1977. Role of the immune response in recovery from Sindbis virus encephalitis in mice. *J. Immunol.* **118**:1070–1075.
- Hasenkrug, K. J., and B. Chesebro. 1997. Immunity to retroviral infection: the Friend virus model. *Proc. Natl. Acad. Sci. USA* **94**:7811–7816.
- Heller, E., and D. H. Pluznik. 1984. Chromosomal assignment of two murine genes controlling susceptibility to spleen focus formation by Rauscher leukemia virus. *Exp. Hematol.* **12**:645–649.
- Ikeda, H., F. Laigret, M. A. Martin, and R. Repaske. 1985. Characterization of a molecularly cloned retroviral sequence associated with Fv-4 resistance. *J. Virol.* **55**:768–777.
- Jacoby, R. O., P. N. Bhatt, and D. G. Brownstein. 1989. Evidence that NK cells and interferon are required for genetic resistance to lethal infection with ectromelia virus. *Arch. Virol.* **108**:49–58.
- Johnston, R. E., and C. J. Peters. 1996. Alphaviruses, p. 843–898. In B. N. Fields, D. M. Knipe, and P. M. Howley (ed.), *Fields/Virology*, 3rd ed. Lippincott-Raven Publishers, Philadelphia, Pa.
- Kozak, C. A., N. J. Gromet, H. Ikeda, and C. E. Buckler. 1984. A unique sequence related to the ecotropic murine leukemia virus is associated with the Fv-4 resistance gene. *Proc. Natl. Acad. Sci. USA* **81**:834–837.
- Meruelo, D., M. Offer, and N. Flieger. 1981. Genetics of susceptibility for radiation-induced leukemia: mapping of genes involved to chromosomes 1, 2, and 4, and implications for a viral etiology in the disease. *J. Exp. Med.* **154**:1201–1211.
- Meruelo, D., M. Offer, and A. Rossomando. 1983. Induction of leukemia by both fractionated x-irradiation and radiation leukemia virus involves loci in the chromosome 2 segment H-30-A. *Proc. Natl. Acad. Sci. USA* **80**:462–466.
- Meruelo, D., and A. Rossomando. 1986. A molecular and genetic approach to understanding the mechanisms by which fractionated X-irradiation induces leukemia in mice. *Leukoc. Res.* **10**:819–832.
- Monteyne, P., J. F. Bureau, and M. Brahic. 1997. The infection of mouse by Theiler's virus: from genetics to immunology. *Immunol. Rev.* **159**:163–176.
- Mullis, K. B., and F. A. Faloon. 1987. Specific synthesis of DNA in vitro via a polymerase-catalyzed chain reaction. *Methods Enzymol.* **155**:335–350.
- Risser, R., and D. Kaehler. 1985. Susceptibility to Abelson or Moloney murine leukemia viruses. *Curr. Top. Microbiol. Immunol.* **122**:162–168.
- Risser, R., D. Kaehler, and W. W. Lamph. 1985. Different genes control the susceptibility of mice to Moloney or Abelson murine leukemia viruses. *J. Virol.* **55**:547–553.
- Risser, R., M. Potter, and W. P. Rowe. 1978. Abelson virus-induced lymphomagenesis in mice. *J. Exp. Med.* **148**:714–726.
- Scalzo, A. A., N. A. Fitzgerald, A. Simmons, A. B. La Vista, and G. R. Shellam. 1990. Cmv-1, a genetic locus that controls murine cytomegalovirus replication in the spleen. *J. Exp. Med.* **171**:1469–1483.
- Scalzo, A. A., N. A. Fitzgerald, C. R. Wallace, A. E. Gibbons, Y. C. Smart, R. C. Burton, and G. R. Shellam. 1992. The effect of the Cmv-1 resistance gene, which is linked to the natural killer cell gene complex, is mediated by natural killer cells. *J. Immunol.* **149**:581–589.
- Scalzo, A. A., P. A. Lyons, N. A. Fitzgerald, C. A. Forbes, and G. R. Shellam. 1995. The BALB.B6-Cmv1r mouse: a strain congenic for Cmv1 and the NK gene complex. *Immunogenetics* **41**:148–151.
- Scalzo, A. A., P. A. Lyons, N. A. Fitzgerald, C. A. Forbes, W. M. Yokoyama, and G. R. Shellam. 1995. Genetic mapping of Cmv1 in the region of mouse chromosome 6 encoding the NK gene complex-associated loci Ly49 and musNKR-P1. *Genomics* **27**:435–441.
- Shifman, M. I., and D. G. Stein. 1995. A reliable and sensitive method for non-radioactive Northern blot analysis of nerve growth factor mRNA from brain tissues. *J. Neurosci. Methods* **59**:205–208.
- Stoflet, E. S., D. D. Koeberl, G. Sarkar, and S. S. Sommer. 1988. Genomic amplification with transcript sequencing. *Science* **239**:491–494.
- Stoye, J. P. 1998. Fv1, the mouse retrovirus resistance gene. *Rev. Sci. Tech.* **17**:269–277.
- Super, H. J., K. J. Hasenkrug, S. Simmons, D. M. Brooks, R. Konzek, K. D. Sarge, R. I. Morimoto, N. A. Jenkins, D. J. Gilbert, N. G. Copeland, W. Frankel, and B. Chesebro. 1999. Fine mapping of the Friend retrovirus resistance gene, Rfv3, on mouse chromosome 15. *J. Virol.* **73**:7848–7852.
- Thach, D. C., T. Kimura, and D. E. Griffin. 2000. Differences between C57BL/6 and BALB/cBy mice in mortality and virus replication after intranasal infection with neuroadapted Sindbis virus. *J. Virol.* **74**:6156–6161.
- Tucker, P. C., D. E. Griffin, S. Choi, N. Bui, and S. Wesselingh. 1996. Inhibition of nitric oxide synthesis increases mortality in Sindbis virus encephalitis. *J. Virol.* **70**:3972–3977.
- Tucker, P. C., E. G. Strauss, R. J. Kuhn, J. H. Strauss, and D. E. Griffin. 1993. Viral determinants of age-dependent virulence of Sindbis virus for mice. *J. Virol.* **67**:4605–4610.
- Varet, B., A. Cannat, and S. Gisselbrecht. 1977. Genetic control of antinuclear antibodies in mice infected with Rauscher leukemia virus. *Cancer Res.* **37**:1115–1118.